Journal of Drug Delivery Science and Technology 65 (2021) 102689

Contents lists available at ScienceDirect

Journal of Drug Delivery Science and Technology

journal homepage: www.elsevier.com/locate/jddst

Combating cancer by utilizing noble metallic nanostructures in combination with laser photothermal and X-ray radiotherapy

Zahra Kayani [a,b,*], Negar Islami [a], Niloufar Behzadpour [a,b], Niloofar Zahraie [a,b], Sanaz Imanlou [c], Paria Tamaddon [a,b], Fatemeh Salehi [a,b], Fatemeh Daneshvar [a,b], Ghazale Perota [a,b,d], Elmira Sorati [b], Sahar Mohammadi [a,b,e], Naghmeh Sattarahmady [a,b,**]

[a] Nanomedicine and Nanobiology Research Center, Shiraz University of Medical Sciences, Shiraz, Iran
[b] Department of Medical Physics, School of Medicine, Shiraz University of Medical Sciences, Shiraz, Iran
[c] Department of Materials Science and Engineering, Shiraz University, Shiraz, Iran
[d] Medical Physics Department, Shahid Sadoughi University of Medical Sciences, Yazd, Iran
[e] Department of Radiologic Technology, Behbahan Faculty of Medical Sciences, Behbahan, Iran

ARTICLE INFO

Keywords:
Near-infrared (NIR)
Photothermal therapy (PTT)
Radiotherapy (RT)
Metallic nanoparticles
Cancer

ABSTRACT

Conventional cancer therapy often fails for an insufficient therapeutic outcome, tumor heterogeneity, and drug resistance. The past decade has witnessed that combination therapies using near-infrared (NIR) light-mediated photothermal therapy (PTT) with its great capacity of heat ablation in tumor tissue enhanced the efficacy of radiotherapy (RT) and reduced radiotoxic effects on normal tissue. Metallic-nanoplatforms, such as transition metal dichalcogenides, gold, copper and, platinum nanoparticles have attracted lots of attention in nano biomedicine. Because of their desired properties such as tunable surface plasmon resonance (SPR), high plasmonic photothermal activity, and high-Z number with stronger photoelectric effects could serve as photosensitizers, and radiosensitizers to improve the efficacy of PTT and RT. Dual radiation of laser light and X-ray into metallic-nanoplatforms considerably improved the cancer treatment via reactive oxygen species (ROS) production. Metallic-nanoplatforms can act as a dual absorber of laser light and X-ray, a common sensitizer, for treatment of cancer. Therefore, in this review, we tried to summarize the developing metallic-nanoplatforms in PTT, RT, and combination therapy.

1. Introduction

At present, surgical procedures, radiotherapy (RT), and, chemotherapy are the main traditional therapeutic approaches for cancer [1–4]. The outcome of traditional treatment is limited due to the non-specific toxicity for both cancerous and normal cells. Drug resistance is another possibility that can be developed during the cancer treatment course and hampers the overall efficacy [5]. Therefore, it is vital to design a specific delivery platform to reduce side effects and get better therapeutic efficacy at lower tolerance. New option in therapy such as hyperthermia with controllable, and noninvasive properties in tumor therapy, has attracted significant interest at the end of the nineteenth century [6]. Hyperthermia can be utilized lonely or more frequently in combination with conventional therapeutic approaches such as chemotherapy, and radiation therapy [7]. As an emerging therapeutic approach, light-triggered therapy has divided into two categories of photodynamic therapy (PDT), and photothermal therapy (PTT). PTT with utilizing 700–1100 nm near-infrared (NIR)-laser in the presence of photoabsorption agents can cause irreversible harm in cancer cells with heat production [8].

NIR laser sources are perhaps the single most diverse category of solid-state lasers; with IR laser diodes, diode-pumped solid-state (DPSS) lasers, flash lamp pumped solid-state lasers and fiber lasers all emitting in the IR laser spectrum [9].This process has some advantages such as selective local therapy by reducing the side effects, simple performance, low difficulty, and quick recovery [9]. However, PTT alone could not

* Corresponding author. Nanomedicine and Nanobiology Research Center, Shiraz University of Medical Sciences, 6th Floor, Administration Building of Shiraz University of Medical Sciences, Zand St., Shiraz, 71348-14336, Iran.
** Corresponding author. Nanomedicine and Nanobiology Research Center, Shiraz University of Medical Sciences, 6th Floor, Administration Building of Shiraz University of Medical Sciences, Zand St., Shiraz, 71348-14336, Iran.
E-mail addresses: kiani_za@sums.ac.ir, kayanizd@yahoo.com (Z. Kayani), nsattar@sums.ac.ir, sattarahmady@yahoo.com (N. Sattarahmady).

https://doi.org/10.1016/j.jddst.2021.102689
Received 26 February 2021; Received in revised form 26 May 2021; Accepted 30 June 2021
Available online 1 July 2021
1773-2247/

completely eliminate tumors, mainly the deep tumors, as a NIR laser intensity decrease in a depth-dependent manner [9]. These limitations may still result in incomplete elimination of cancer cells, which in turn lead to tumor recurrence and metastasis [9]. Indeed, PTT in combination with other therapeutic approaches could improve therapeutic effectiveness. Radiation therapy (RT), without depth restriction, ionizing radiation (e.g., γ-rays, X-rays) has traditionally been one of the routine treatments of cancer, and other diseases. X-ray is an electromagnetic radiation of extremely short wavelength and high frequency, with wavelengths ranging from about 10^{-8} to 10^{-12} m and corresponding frequencies from about 10^{16} to 10^{20} Hz (Hz) [10]. RT with ionizing radiation locally causes lethal damage to cancer cells, through oxygen-centered radicals, which made damages in DNA [10]. The negative point that severely hindered the clinically applied RT is hypoxia-induced radiation resistance in some tumors and high-dose ionizing radiation may cause damage in healthy tissues around the tumor, and resulting in a toxicity effect [11]. To solve this obstacle, in recent years, it has exploited various strategies based on radiosensitizer to avoid the radioresistance, to overcome hypoxia-tumor RT, and reduced the ionizing radiation dose, and severe side effects to bordering healthy tissues [11,12]. A certain level of PTT-induced hyperthermia is a modifier of intra-tumoral blood flow, and increased oxygenation of the tumor microenvironment, which may enhance the sensitivity of cancer cells to RT. Therefore, this new combined treatment based on PTT and RT may shed light on cancer therapy [13]. Various nanoagents have been used in PTT, which displayed great anticancer and antibacterial effects. For instance, carbon and polypyrrole are the recent materials with different combinations showing remarkable anticancer and antipathogenic efficiency [14–19]. They are not only sensitive to NIR light but also sensitive to ultrasound, a novel approach to battle cancer [17,20]. Metallic nanoplatforms such as gold [21,22], silver [23,24], silica [25], copper [26], platinum [27], and ferrite [28] have noticed as desirable agents for medicinal approaches such as PTT, and RT. Among different photosensitizers, and radiosensitizer, metallic nanomaterials, represented surface plasmon resonance (SPR) upon excitation of the surface electrons at their resonance frequency, and release Auger electrons in response to external beam X-ray radiation [29,30]. The SPR effect of nanomaterials depends on various factors such as type, size, shape, composition, dielectric constant, and the surrounding medium [31]. Achieving nanostructures with biocompatibility, less damage, high photoconversion efficiency, and radiosensitization effect has remained an attractive subject for researchers [21,27,32].

The surface modification of nanostructures with the biocompatible polymer can develop effective surface shielding to prolong the blood circulation half-life and enhanced the permeability, retention (EPR) effect, and successful accumulation of nanoparticles (NPs) into the tumor interstitium [33–35]. Metallic nanoplatforms with photothermal, and radiosensitizers properties may play a promising role in a synergistic PTT/RT of cancer cells (Fig. 1) [11,36–38]. Because of more complexity, diversity, and heterogeneity in tumors, main cancer therapeutic approaches such as surgery, RT, chemotherapy, and targeted therapy shifted from common monotherapy toward combination therapy. Achieving the optimized combination therapy may be critical for overcoming tumor-inhibiting mechanisms [8,11]. In this article, we will review the recent research on design, fabrication, and structural characterization of various metallic nanoplatforms, and highlighted their potential capacity in NIR-responsive hyperthermia, and radiosensitization in optimizing the efficacy of cancer treatment.

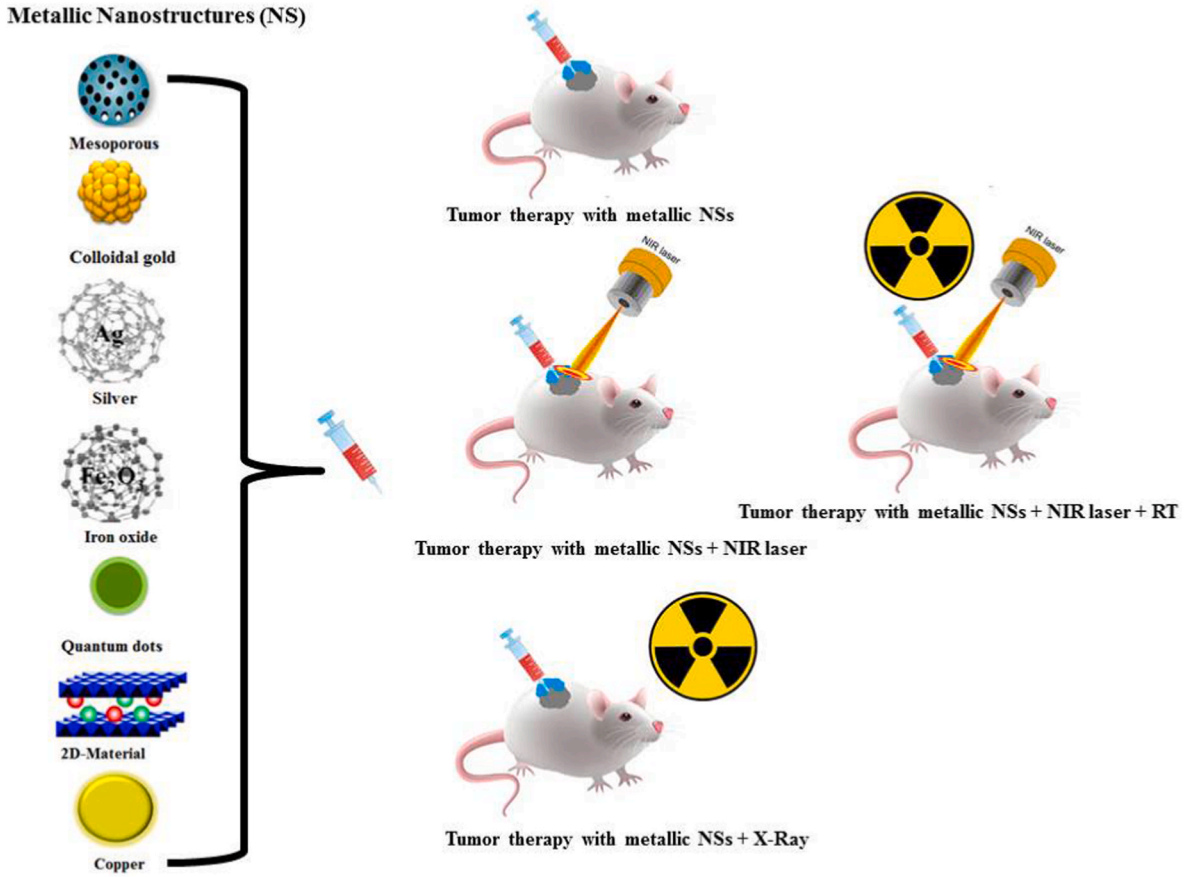

Fig. 1. Different metallic nanostructures are agents sensitizing by laser light and X-ray in photothermal therapy (PTT) and radiotherapy (RT) of cancer.

1.1. Metal-based nanomaterials-in RT, PTT, and combined therapy

1.1.1. Two-dimensional transition metal dichalcogenides (2D TMDs)

Transition metal dichalcogenides (TMDCs) with sandwich architecture have excellent optical, electronic, and magnetic properties. They comprise transition metal atoms such as (Mo, W, Ti, Ta, Zr, V, Nb, etc.) covered with two layers of chalcogen atoms (S, Se, or Te) [39]. Single-layered 2D TMDCs such as molybdenum selenide (MoSe2) with high-Z elements show superior properties, such as strong NIR absorbance, high photothermal conversion efficiency, and good thermal stability offering the potency of being excellent photothermal agents [40–42]. Also, certain types of TMDs with stronger photoelectric effects and high-Z elements such as tungsten disulfide (WS_2), and bismuth selenide (Bi_2Se_3) could serve as a radiosensitizer to achieve effective cancer RT by absorbing X-ray, and concentrating radiation dose within tumors [43–46]. Among TMDs, it predicts that ultrasmall NPs based on tungsten could enter cell nuclei close to the target DNA [47–49]. Yong et al. fabricated lipoic acid-modified polyethylene glycol (LA-PEG) coated WS_2 quantum dots (QDs) based on facile and 'green' procedure through physical grinding, and ultrasonication [49]. WS_2 (QDs) revealed superior properties, such as strong NIR absorbance, high photothermal conversion efficiency ($\eta = 44.3\%$) as well as good X-ray absorption ability offering their potential for a synergistic PTT, and RT of cancer cells. Colony formation assay showed that 4T1 cells incubated with WS_2 enhanced PTT/RT combinational therapy and decreased cell viability to 6%, which was 80.6% lower than that of WS_2+RT and was 84.6% lower than that of WS_2+PTT. It confirms WS_2-dependent synergistic reinforcement of RT/PTT *in vitro*. The most efficient eradication of tumor cells achieved by the mice group treated with WS_2 QDs + NIR + RT while the groups treated only with WS_2+NIR or WS_2+RT induced partial damage on tumor tissues. Thus WS2 QDs could be powerful nanoplatforms for the multimodal image-guided in synergistic PTT/RT [49].

1.2. 2D TMDs nanocomposite

Wang et al. generated the MnO_2 nanoshell on the surface of mesoporous polydopamine nanosponges (MPDA NSs) embedded with WS_2 QDs with multimodal computed tomography (CT)/multispectral optoacoustic tomography (MSOT)/magnetic resonance imaging (MRI) capability, radiation enhancement effect, and excellent photothermal properties [46]. The photothermal efficiency of MPDA-WS_2@MnO_2 NPs was determined to be $\eta = 16.8\%$ under an 808 nm laser. Cytotoxicity assay of 4T1 cells revealed MPDA-WS_2@MnO_2 NPs plus laser irradiation killed a significant portion of cells because of the capability of MPDA-WS_2@MnO_2 NPs to convert NIR light to heat while less cell death observed in laser-only, and MPDA-WS_2@MnO_2 NPs-only groups. Tungsten (W) with a high photoelectric absorbance capacity in MPDA-WS_2@MnO_2 NPs markedly increased the sensitivity of 4T1 cells to X-ray radiation and showed lower percentages of viable cell colonies compared to the control group (X-ray only). MnO_2 components alleviate tumor hypoxia by catalyzing the tumor overexpressed H_2O_2 and considerably enhances RT performance. The photothermal effect of MPDA-WS_2@MnO_2 NPs in 4T1 tumor-bearing MPDA-WS_2@MnO_2 NPs mice under 808 nm NIR laser irradiation (1.5 W cm^{-2}) showed a rapid increase in temperature which reached a plateau about 54 °C in 4 min. Then it resulted in notable heat generation at tumor tissue sufficient to induce irreversible cancer tissue necrosis. The efficacy of combined PTT and RT along with MPDA-WS_2@MnO_2 NPs showed significant inhibition in tumor growth, which was superior to individual therapy and implied the synergistic effect of NIR mediated hyperthermia and RT treatment [46]. Qi et al. prepared folic acid conjugated molybdenum selenide nanosphere coated bovine serum albumin (FA-$MoSe_2$@BSA NSs) as a dual-modality therapy agent for a synergistic PTT/RT [50]. FA-$MoSe_2$@BSA NSs possessed excellent photothermal stability for BSA assembly and PEG coating. After three cycles of NIR irradiation, the photothermal properties were kept with no attenuation in elevation of temperature degrees. Also, FA-$MoSe_2$@BSA NSs have the radio-sensitization ability, which could concentrate X-ray energy inside tumor cells, and released secondary Auger electrons. It caused suppression in tumor cell growth via DNA damaged [51,52]. Combined PTT/RT, could enhance the therapeutic efficiency over 95% *in vitro* with the obvious synergistic therapeutic outcome compared to PTT alone or RT alone along with FA-$MoSe_2$@BSA NSs [50]. Shen and co-authors have prepared ultrathin uniform Rhenium disulfide (ReS_2) nanosheets with PEG surface modification (ReS_2-PEG) through a high-temperature "bottom-proton up" solution method [53]. ReS_2-PEG nanosheets with excellent stability, high NIR absorption, and strong X-ray attenuation ability successfully employed for triple modal photoacoustic (PA), CT, and single photon emission computed tomography (SPECT) imaging on 4T1 tumor-bearing mice. Efficient tumor retention occurred after systemic administration of ReS_2-PEG. These nanosheets as a photothermal agent for NIR triggered tumor hypothermia enhanced the efficacy of RT and led to significant improvement in tumor oxygenation. It could relieve hypoxia-associated radiation resistance of solid tumors, contributing to the remarkable enhanced therapeutic effect in the combined PTT/RT. Therefore, ReS_2-PEG with the ultra-large specific surface area may be used as a multifunctional drug carrier for efficient drug loading and further combination with chemotherapy, and PTT/RT [53]. TMDs based on titanium increases the intra-tumor blood circulation under strong absorbance of NIR laser irradiation and facilitate oxygen availability inside the tumor which can enhance the RT effect. Therefore, they are great PTT, and radiosensitizers agents [53–55].

1.3. Targeted 2D TMDs nanocomposite

In most TMDs surface modification like other nanostructures with a high specific surface area can improve biocompatibility, tumor targeting, prolong blood circulation, and reduce the clearance from the body. In this way, Cao et al. prepared TiS_2-HSA-FA, (nano agents based on titanium disulfide (TiS_2) functionalized with human serum albumin (HSA), and folic acid) to examine PTT effect under NIR laser irradiation (808 nm, 0.8 W cm^{-2}, 5 min) [56]. The highest temperature and photothermal conversion efficiency were 65.3 °C, and ~58.9%, respectively. The photostability was confirmed by being stable throughout five cycles. After 24 h from incubation of CT26 cell with TiS_2-HSA-FA, CCK-8 assay indicated no significant cytotoxicity even at higher concentrations up to 0.8 mg mL^{-1} with 45% of cellular uptake. Moreover, TiS_2-HSA-FA + NIR + RT (NIR; 808 nm laser 0.8 W cm^{-2}, 5 min), and (RT; 5Gy) displayed the highest inhibition rate (93.4%) for CT26 cells through damage in cellular DNA. Also, the energy of X-ray radiation absorbed more effectively by tumor cells and caused a significant inhibition in tumor growth. The synergistic PTT/RT was investigated in tumor-bearing mice, with NIR, and RT (6 $mg.kg^{-1}$of TiS_2). The temperature of the tumor region in (TiS_2-HSA-FA + NIR + RT) group was increased by 25 °C, and remarkable tumor growth inhibition was observed after 21-day of treatment. Since the TiS_2-HSA-FA with good biocompatibility, strong NIR light absorbance, good stability, and notable efficacy as a radio-sensitizer could act as an "all in one" nano agent in cancer therapy [56]. Because of the limited depth penetration of PTT in the NIR-I window (first biological window: 700–900 nm), the recent studies focused on PTT in NIR-II biological window (the second biological window: 1000–1350 nm) which showed more penetration depth, and subsequently better tumor ablation [57–60]. Tang et al. synthesized the 2D multifunctional Ti_3C_2@Au nanocomposites by a chemical exfoliation method [61]. The Ti_3C_2 showed a broad absorption band by the UV–vis–NIR spectrum at 700–1000 nm. The Au growth on the surface of Ti_3C_2 enhanced the absorbance of nanocomposites by increasing the wavelength in both NIR-I and NIR-II, which is favorable for deeper tumor penetration. Photothermal behavior tested under laser irradiation (NIR-II region, 1064 nm) at different concentrations of Ti3C2@Au-PEG solution. The photothermal conversion efficiency of

Ti_3C_2@Au-PEG was better than Ti_3C_2 nanosheets for Au coated on the surface of Ti_3C_2@Au-PEG led to better absorbance. The 4T1 cells treated with Ti_3C_2@Au-PEG + X-ray (6 Gy) showed significant cell death due to DNA damage [61]. A notable increase in temperature of tumor site observed following an intravenous (IV) injection of Ti_3C_2@Au-PEG under laser irradiation (0.75 W cm^{-2}, 1064 nm for 10 min). Then, Tang et al. used the low power density laser to achieve a synergistic effect between PTT, and RT. The tumor hypoxia microenvironment relieved by employing Ti_3C_2@Au-PEG under NIR-II irradiation, which led to mild PTT and better RT efficiency [61]. Therefore, in a group with combined PTT + RT + Ti_3C_2@Au-PEG severe destructions occurred in the tumor area [61]. Also, no significant weight loss observed in mice treated with Ti_3C_2@Au-PEG nanocomposites which can be favorable for *in vivo* application with no noticeable toxicity of Ti_3C_2@Au-PEG nanocomposites. Table 1 summarizes different 2D TMD based nanostructure reported as PTT and RT agents applied on various types of tumor cells *in vitro* and *in vivo*.

1.4. Gold based nanostructures

Since 1950 Gold-based nanostructures have attracted great attention in nano biomedicine for low toxicity, biocompatibility, tunable surface plasmon resonance (SPR), oxidation resistance, easy surface modification, high plasmonic photothermal activity. Allocated promising therapeutic opportunities of gold-based nanostructures have been investigated for approval in clinical trials [62–65]. Gold nanostructures are widely studied in cancer diagnostics [66], intracellular imaging [67], biological sensing [68,69], drug, and gene delivery [70]. Gold nanostructures with different shapes, sizes, and compositions could be utilized as excellent photothermal and radiosensitizer agents in PTT and RT [71–73].

Heidari et al. prepared gold-ferrite nanocomposite (GFNC) for simultaneous diagnostic, and treatment purposes of melanoma cancer [74]. This nanostructure showed the ability to destroy B16F0 melanoma tumors in mice upon 808 nm light irradiation [74].

Also, a nanocomposite of PEG-curcumin-gold nanoparticles (PEG-Cur-Au NPs) with 808 nm absorption was designed and showed a remarkable anticancer effect on the C540 (B16/F10) cells, and melanoma in tumor-bearing mice [73]. A gold/manganese dioxide nanostructure (nano-gold elements stuck on manganese dioxide nanorods) (Au/MnO2 NC) was applied as a PTT agent which showed PTT efficiency (η: 26.1%) and destroying effect on the C540 (B16/F10) cells, and melanoma animal models, upon 808-nm laser irradiation [21]. Gold nanostructures with their outstanding properties in X-ray attenuation as well as high Z number are widely investigated in CT and RT [75–77]. The radiosensitizing effect depends on the size and bigger nano-elements would reveal better efficiency. For instance, the 50 nm gold nanoparticles have shown a stronger radiosensitizing ratio and

Table 1
Summary of recent advancements of different Two-Dimensional Transition Metal Dichalcogenides (2D TMDs) based nanostructures reported as PTT and RT and characteristics of testing (NP type, cells, and tumor).

Two-Dimensional Transition Metal Dichalcogenides (2D TMDs)						
Type	**NPs size**	**Laser**	**η**	**RT**	**Therapeutically effect**	*Ref.*
Tungsten disulfide quantum dots (WS_2 QDs) into mesoporous polydopamine nanosponges (MPDA NSs with manganese dioxide (MnO_2) (MPDA-WS_2@MnO_2)	~170 nm	*in vitro* & *in vivo*: (1.5 W.cm^{-2}, 5 min, 808 nm)	16.8%	*in vitro*: 160 kev, (0, 2, 4 and 6 Gy), 2.012 Gy min^{-1}; *in vivo*:6 Gy	A significant portion of 4T1 cells killed with MPDA-WS_2@MnO_2 NPs + PTT due to conversion of NIR light to heat. Remarkable inhibition in tumor growth was observed in mice treated with combined PTT + RT along with MPDA-WS_2@MnO_2 NPs, which was implied the synergistic effect of NIR mediated hyperthermia and RT treatment.	[46]
Tungsten Sulfide (WS_2) quantum dots (QDs) (WS_2 QDs)	3 ± 0.18 nm	*in vitro* (0.3, 0.5, 1.0 W.cm^{-2}) for 10 min, 808 nm; *in vivo:*(1 W.cm^{-2}, 10 min, 808 nm)	44.3%	*in vitro*: (0, 2, 6 and 8 Gy); *in vivo*:6 Gy	4T1 cell viability drastically inhibited to 6% via induction of apoptosis by WS2 QDs enhanced PTT/RT of cancer cells Thoroughly elimination of tumor was achieved by the treatment of WS_2 QDs + NIR + RT.	[49]
Molybdenum selenide nanodots ($MoSe_2$ NDs) and bovine serum albumin (BSA) assembled nanospheres ($MoSe_2$@BSA NSs)	30 nm	*in vitro* & *in vivo*: (1 W.cm^{-2}, 5 min, 808 nm)	(–)	*in vitro:* 0–5 Gy, 0.084 Gy/s), *in vivo*: (5 Gy)	The most significant concentration-dependent cell death, with 92.8% suppression rate due to the photothermal ablation of PTT and DNA damage by RT of FA-$MoSe_2$@BSA NSs. FA targeting enhanced the 4T1 cell internalization of FA-$MoSe_2$@BSA NSs observed in FA-$MoSe_2$@BSA NSs + NIR + RT-treated group. The most remarkable 4T1-tumor growth inhibition was observed in combined PTT + RT + FA-$MoSe_2$@BSA NSs, achieving an obvious synergistic therapeutic outcome in comparison to PTT alone or RT alone delivered by FA-$MoSe_2$@BSA NSs.	[50]
Rhenium disulfide (ReS_2) nanosheets surface modified with poly (ethylene glycol) (PEG) (ReS_2-PEG nanosheets)	~10 nm	*in vitro*: (0.8 W. cm^{-2}, 5 min, 808 nm); *in vivo:* (0.6 W. cm^{-2}, 20 min, 808 nm)	(–)	*in vitro:* (6, 4, 2, 0 Gy); *in vivo*:6 Gy	ReS_2-PEG nanosheets combined with PTT + RT conducted remarkable destruction in 4T1 tumors due to synergistic therapeutic effects.	[53]
Nanoagent based on titanium disulfide (TiS_2), human serum albumin (HSA), and folic acid (FA), (TiS_2-HSA-FA)	135.3 nm	*in vitro* & *in vivo:* (0.8 W. cm^{-2}, 5 min, 808 nm)	~58.9%	*in vitro* & *in vivo*: 5Gy	TiS_2-HSA-FA under NIR + RT treatment displayed the highest CT26 cell inhibition rate (93.4%) and the best tumor growth inhibition has seen due to synergistic therapeutic outcome.	[56]
Titanium carbide@gold nanocomposite (Ti_3C_2@Au nanocomposites)	~200 nm	*in vitro:* (0.4, 0.6, and 0.75 W. cm^{-2}, 5 min, 1064 nm); *in vivo*: (0.75 W. cm^{-2}, 10 min, 1064 nm)	39.6% in 1064 nm & 34.3% in 808 nm	*in vitro* & *in vivo*: 6 Gy	The Ti_3C_2@Au-PEG nanosheets killed cancer cells under the 1064 nm NIR-II laser and under X-ray showed salient DNA damage. The most obvious tumor growth inhibition was found in PTT/RT + Ti_3C_2@Au-PEG through a synergistic therapeutic effect.	[61]

Abbreviations: NIR, near-infrared; NP, nanoparticle; Ns, nanostructure; PTT, photothermal therapy; RT, radiotherapy.

cellular uptake. *In vivo*, and *in vitro* exploration have revealed that the improvement of radiation effects for the 12, and 27 nm PEG-coated gold nanoparticles with prolonged blood circulation were higher than the 4.8, and 46.6 nm ones [75,78–80]. For, PTT more new shapes of nanostructures were designed. In gold nanoparticles altering the spherical structure to spiky shapes or superstructures, the absorption wavelength could be shifted from visible to NIR region. Also, the tips in spiky provide a higher local electromagnetic field [81,82]. All these features represent a successful nomination of AuNPs in PTT/RT combined therapy. First, in 2016 Ma et al. designed hollow and spike-like gold nanostructures by a facile galvanic replacement reaction [83]. Gold nano spikes (GNSs) exhibited low cytotoxicity and high photothermal conversion efficiency ($\eta = 50.3\%$) with excellent photostability. In the colony formation assay illustrated that GNS-mediated PTT and RT decreased the cell survival rate to 89%, and 54%, respectively. While survival rates of cells decreased to 40% in the combined PTT/RT that could be related to an increase in the sensitization enhancement ratio (SER) of GNS. Tumor growth study showed that in the mice model group the tumor growth inhibition reached 92.2%, in comparison to the group treated with the GNS-enhanced X-ray radiation (TGI = 29.8%) or the group treated with the GNS-mediated PTT (TGI = 70.5%). The synergistic cancer treatment performance assigned to the effect of hyperthermia, which effectively improved the radiosensitizing effect of hypoxia in cancer cells that were resistant to ionizing radiation [83]. Moreover, it has also been proved that hybrid bimetallic nanoparticles exhibit better optical and chemical properties than those of single element-containing nanoparticles. Hence, combining Pt and Au nanostructure together reveals good photostability and high photothermal conversion efficiency in PTT for cancers. Liu et al. were rationally designed and fabricated PEGylated Au@Pt nanodendrites (NDs) [84]. Au@Pt nanodendrites exhibited broad absorbance in the NIR region with the growth of Pt nano branches. It also showed a good radiosensitizing effect due to the composition of Au and Pt that improved annihilation impacts of RT via inducing a highly localized radiation dose within cancer cells. More significantly, the mixture of Au@Pt NDs + RT + PTT stopped 4T1 cells growth to 30%, which was 42% lower than the effect of Au@Pt NDs + PTT individually, and 25% lower than the result of Au@Pt NDs + RT alone. However, the Au@Pt NDs with significant CT imaging signal improvement at low NIR laser power, and X-ray radiation dose through the synergistic effect of PTT/RT could provide stronger theranostic nano-platform for cancer diagnosis, and therapy [84]. Targeted photodynamic therapy based on noble metals is an appropriate way to the kill abnormal and cancerous cells [85,86]. Capabilities of two types of Fe IONPs with different shells and functionalized structures are combined with Au NPs, in the field of cancer hyperthermia explored by Hosseini et al. [87]. RT or PTT individually causes cell ablation by necrosis, accidental cell death, but [combining all three methods together NPs ($Au@Fe_2O_3$), PTT, and RT] caused 51% apoptosis in KB cells [87–89]. Then, the therapeutic effect of the synthesized $Au@Fe_2O_3$ NPs in combination with 6 MV X-ray, and NIR laser effectively induced cell death in the KB cell line while in [nanoparticles + PTT] group or [nanoparticles + RT] group declined the cell viability to ~40%. $Au@Fe_2O_3$ NPs are a promising candidate to trigger apoptosis in the process of photo-thermo-radiotherapy of cancers. Parchur et al. fabricated $Au@Gd_2O_3$:Ln (Ln = Yb/Er) (TNPs) as optical/MR/X-ray contrast agent for interventional image-guided PTT of solid tumors [90]. Following systemic administration, TNPs were deposited in tumors via enhanced permeation, and retention effect, but the delivered dose to tumors was typically low; to overcome this adverse impact TNPs were infused into the liver of tumor-bearing rats. By inserting a 100-μm fiberoptic carrying 808-nm light for 3 min under DynaCT image guidance photothermal ablation was performed, and Showed local destruction through hyperthermia around tumor vicinity and minimum injury to the adjacent liver tissue [90].

1.4.1. Targeted gold based nanostructures

Herein, Keyvan Rad et al. introduced photoresponsive gold-decorated polymer nanoparticles (PGPNPs) with surface-modified folic acid (FAPGPNPs) as a site-specific tumor cell targeting agent, and improved intracellular uptake via endocytosis [91]. FAPGPNPs with strong surface plasmon resonance (SPR) absorption and superior local photothermal efficiency under NIR at 808 nm have been applied for efficient, targeted photodynamic, and PTT in rats with brain tumors (C6 glioma). Cellular uptake for FAPGPNPs was 71.8% while for the nonconjugated ones was 28.8% [91]. FAPGPNPs showed an increment in cell destruction of the treated C6 rat glioma cancer cells via enhanced ROS photogeneration under UV irradiation (365 nm), as an efficient method for cell death, and cancer therapy. For this reason, FAPGPNPs as promising multifunctional smart nanoprobes could be used in targeted photodynamic, and PTT of cancer cell ablation with less nonspecific damages, and selectively cell line labeling [91]. Likewise, ^{177}Lu–Au-NLS-RGD-Aptamer antiangiogenic nanosystem with photothermal, and the radiotherapeutic effects were evaluated on U87MG cancer cells to assess the synergic effect of both therapies [92]. The cell viability decreased to 2.14 ± 0.27% for the synergistic effect of its photothermal, and radiotherapeutic properties, the ^{177}Lu–Au-NLS-RGD-Aptamer nano-radio-pharmaceutical which was correlated with the *in vivo* tumor growth inhibition response observed in mice with U87MG-induced tumors. In brief, one nano-radio-pharmaceutical platform with synergistic radio, and thermotherapy effect could be potentially useful in cancer treatment [92]. Neshastehriz et al. prepared folate conjugated gold nanoparticles (F-AuNPs) to search about their effects in a synergistic therapy of mouth epidermal carcinoma cells by combining PTT, and RT [88]. Cell viability of KB cells incubated with F-AuNPs, at a simultaneous exposure of laser, and X-ray significantly decreased while laser irradiation or NPs solely showed no cell ablation. Results showed that the F-AuNPs as promising, and research-valuable nanoconjugate in targeted photo-thermo-radiotherapy of cancer [88]. Li et al. were employed preloaded Berberine (Ber) into folic acid targeting Janus gold mesoporous silica nanocarriers (FA-JGMSNs) as radiosensitizing, and photothermal agents for liver cancer therapy [93]. FA-JGMSNs with a high drug loading capacity released Ber in response to a tumor microenvironment and showed a prolonged Ber intracellular retention, thus improved its therapeutic efficiency. Also, FA-JGMSNs showed the stronger killing of SMMC-7721 cells in dual-therapy (RT + NIR) compared to monotherapy RT or NIR. Notably, FA-JGMSNs with excellent antitumor efficacy in combination with PTT/RT didn't have a toxic effect on HL-7702 cells, showing excellent biosafety of the triple-model therapy. Hence, the triple-model therapy (FA-JGMSNs-Ber + RT + NIR) *in vivo* showed a higher level of tumor-growth inhibition than FA-JGMSNs-Ber or FA-JGMSNs + RT or JGMSNs-Ber + RT + NIR. These findings indicated that FA-JGMSNs with no adverse effect on healthy tissue would be a promising candidate for multidimensional therapies of liver cancer [93]. Dual-targeted gold nanoprisms compromised gold nanoprisms (Au NPR) conjugated to phenanthroline derivatives functionalized tetraphenylethene (TPE) with Zn (Au-Apt-TPE@Zn) were utilized for dual-modal imaging, and precise cancer PTT [94]. Synthesized Au-Apt-TPE@Zn exhibited the cell to selective nuclear -targeted ability by nanoparticle surface decoration with an AS1411 DNA aptamer. Au-Apt-TPE@Zn irradiated by laser revealed significant hyperthermia effect against SGC-7901 cells growth by inducing apoptosis through triggering overproduction of reactive oxygen species (ROS) and regulating multiple signal crosstalk. Also, *in vivo* investigations showed deep penetration, with a strong photothermal impact against gastric carcinoma xenograft that inhibited tumor growth by activation of the apoptosis pathway [94]. Table 2 summarizes different gold based nanostructure reported as PTT and RT agents applied on various types of tumor cells *in vitro* and *in vivo*.

Table 2
Summary of recent advancements of different gold based nanostructures reported as PTT and RT and characteristics of testing (NP type, cells, and tumor).

Gold based nanostructures						
Type	**NPs size**	**Laser**	**η**	**RT**	**Therapeutically effect**	*Ref.*
Hollow and spike-like gold nanostructures (GNSs)	54 ± 9 nm	*in vitro*: (2 W. cm^{-2}, 10 min, 808 nm); *in vivo*: (0.75 W. cm^{-2}, 5 min, 808 nm)	50.3%	*in vitro* & *in vivo*: 4 Gy	Colony formation assay of KB cells clearly demonstrated that GNS-mediated PTT and RT reduced the cell survival fraction to 89% and 54%, respectively. Tumor growth inhibition (TGI) in the synergistically treated U14 tumor-bearing mouse group reached 92.2%, which was much higher than that of the group treated with the GNS-enhanced X-ray radiation (TGI = 29.8%) or the group treated with the GNS-mediated photothermal therapy (TGI = 70.5%).	[83]
PEGylated Au@Pt Nanodendrites (PEGylated Au@Pt NDs)	~30 nm	*in vitro*: (1 W cm^{-2}, 10 min, 808 nm)	(−)	*in vitro*: 4 Gy	Synergistic effect of PTT/RT combinational therapy enhanced by Au@Pt NDs and declined the cell viability of 4T1 to 30%.	[84]
Gold coated iron oxide nanoparticle (Au@Fe_2O_3 NP)	~50 nm	*in vitro*: (6 W cm^{-2}, 10 min, 808 nm); *in vivo*: (0.75 W. cm^{-2}, 5 min, 808 nm)	(−)	*in vitro*: 6 mv, 2 Gy	The cell viability of KB cells treated with Au@Fe_2O_3 NP + PTT + X-ray substantially decreased and likely relates to ROS production and subsequent induction of apoptosis.	[87]
Theranostic nanoparticles (TNPs) composed of PEGylated Au@Gd_2O_3:Ln (Ln = Yb/Er) (PEGylated TNPs)	~75 nm	*in vivo*: (0.50 and 0.55 W. cm^{-2}, 5 min, 808 nm)	55.7%	(−)	TNPs in rats bearing colorectal liver metastasis (CRLM) can be effectively employed for the site directed PTT.	[90]
Folate-conjugated (photoresponsive gold-decorated polymer nanoparticles (PGPNPs).) (FA-PGPNPs)	40−60 nm	*in vitro:* (0.8 W cm^{-2}, 14 min, 808 nm);	(−)	(−)	FA-PGPNPs reveals the efficient role in targeted PTT due to noticeable elevation of temperature from 25 to 86 °C during NIR laser exposure for the C6 glioma cells -treated FA-PGPNP samples within 14 min revealed, whereas the with cell culture medium (as control) displayed no obvious temperature change.	[91]

Abbreviations: NIR, near-infrared; NP, nanoparticle; Ns, nanostructure; PTT, photothermal therapy; RT, radiotherapy.

1.5. Platinum based nanostructure

Platinum (Pt) as noble metal exhibits significant antioxidative capacity, biological stability, catalytic activity, damage to DNA, antineoplastic effect, and fascinating optical property [37,95–98]. Platinum nanoparticles (Pt NPs) and their alloys as a new platform have been applied in various approaches such as electrocatalysis, electronic devices, (bio) sensors, bone allograft, dentistry, and tumor cell killing [99–105]. Platinum nanostructures with both reported cytotoxicity and biocompatibility compared to the chemotherapeutic drugs, such as cisplatin can increase the level of glutathione, superoxide dismutase activity, and malondialdehyde in cancer cells similar to the treatment of hepatocellular carcinoma induced by diethylnitrosamine in rats [106]. While the 50% cytotoxic concentration (CC50) values of 2.904, and 6.829 mg mL^{-1} reported toward HepG-2, and MCF-7 cell lines confirming the biocompatibility of Pt NPs [107]. Potent anticancer activities of Pt NPs have observed on various cancer cell lines such as epidermoid (A431), breast (MCF-7), and cervical carcinoma (SiHa, and HeLa) [108]. Pt NPs exhibited extreme thermal stability and no indications of distortions even when the temperature increased up to 700 °C. Also, Pt NPs displayed light absorption in the second biological window which made them effective photosensitizers in PTT of cancer cells [109,110]. The photothermal properties and cell compatibility of Pt NPs depend on their shape, size, and crystalline structure [109]. Pt NPs have various shapes such as cubes, octahedrons, cuboctahedrons, tetrahedrons, nano worms, and spherical [111,112]. The toxicity/biocompatibility of five different sized/shaped Pt NPs within a narrow size regime of 1–21 nm was investigated based on their interaction with Neuro 2 A cell lines [113]. From five groups of Pt NPs, the group with sizes ranging from 5 to 6 nm had distinct non-cytotoxic properties while all the others revealed different extents of cytotoxicity. These Pt NPs with sizes 5–6 nm with the superior property of no cytotoxicity were employed for the promising PTT of Neuro 2 A cells. Pt NPs in the presence of NIR 1064 nm laser irradiation could increase 9 °C in the temperature which triggering cell ablation through the beginning of an apoptosis pathway and leading to the effective photothermal killing of cancer cells [109]. Pt NPs, as a high-Z radio-sensitizing component, can enhance the radiation dose at the target area by inducing more occurrences of photoelectric process, and pair production through interactions with X-ray, and precise conformity of radiation dose [113]. In combination therapy, Pt NPs are applied to develop the synergetic impact of NIR radiation, and x-ray to defeat the resistance of platinum drugs, and systemic toxicity in comparison with PTT, RT, and chemotherapy alone. Daneshvar et al. reported the effect of spherical Pt NPs with a diameter of 12.2 ± 0.7 nm in the treatment of melanoma cancer [27]. Pt NPs showed photothermal conversion activity in a concentration-dependent manner. Pt NPs induced cell death (>50%) in B16/F10 cells treated with 250 μg mL^{-1} of Pt NPs in presence of 808-nm laser light radiation at both power densities (1.0, and 1.5 W cm^{-2}). Upon X-ray radiation, after 72 h a significant decrease in the viability of B16/F10 treated with 250 μg mL^{-1} of Pt NPs was observed which were 29.8%, 27.3%, and 13.7% at dose radiation of 2, 4, and 6 Gy, respectively. Viability of 82.8% appeared for sole Pt NPs (at the same concentration), and 49.7%, 42.9%, and 39.2% were for sole X-ray at dose radiation of 2, 4, and 6 Gy, respectively. Laser light radiation in combination with RT into the cells incubated with Pt NPs led to deeper treatment with cell viability ~15% through more ROS production, compared with sole laser radiation or X-ray illumination. Therefore, combining laser light, and X-ray radiation based on Pt NPs reached a remarkable synergistic effect superior to the respective individual therapies [27]. Salehi et al. fabricated a platinum mesoporous nanostructure (Pt MN) with a sponge architecture comprising tiny adhered particles of <11 nm, and about 5-nm pores [114]. Pt MN represented NIR and X-ray absorbance with considerable cellular uptake in a concentration range of 10–100 μg mL^{-1} and toxicity in a dose-dependent manner [114,115]. The increased cytotoxicity reported for Pt MN was for its mesoporous structure similar to mesoporous ruthenium [116], carbon [117,118], and magnesia [119]. The viability of C540 (B16/F10) cells treated with PT MN upon NIR irradiation (at a power density of 1.0, and 1.5 W cm^{-2}) reached 53, and 40%. But under X-ray irradiation at a dose of 2, 4, and 6 Gy, the cell viability considerably decreased to 15.8 and 4.0% after 24 h, and 72 h, respectively. Thus, Pt MN could be an effective radiosensitizer for enhancing the RT efficacy. Pt MN in combined therapy with PTT/RT interestingly led to cell death in melanoma cancer cells (~99%). This significant decrement in cell viability in combined therapy caused by reactive oxygen species (ROS) production along with heat generation upon laser light radiation. Thus, Pt MN with thermoradioensitizing property and drug loading capability owing to its

porous structure could be promising nanoplatforms in cancer therapy [114]. Ma et al. synthesized uniform worm-like platinum nanoparticles (Pt nano worms) coated with poly (maleic anhydride-alt-1-octadecene)-PEG (C18PMH-PEG) (PEG-Pt nano worms) in a facile way [112]. It showed high photothermal conversion efficiency of about 38.9% which was higher or comparable to that of the most reported photothermal reagents. Biocompatible Pt nano worms combined with 1064-nm laser (0.75 W cm^{-2}, 5 min), led to necrocytosis by hyperthermia in 4T1 breast cancer cells while only laser irradiation or the nano worms could not induce any cell death. X-ray attenuation ability of the Pt nano worms offers this nano agent as excellent radio-sensitizers. Colony-forming unit (CFU) assay exhibited the group incubated with the Pt nano worms regardless of the X-ray dose was effective in enhancing the RT effect. The integrated Pt nano worms used with a low-powered 1064 nm laser (0.6 W cm^{-2}, 10 min) improve the oxygen supply in tumor tissue, and efficient tumor shrinkage was observed along with X-ray (6 Gy) irradiation while the normal tissues were unaffected in murine.

1.5.1. Targeted platinum based nanocomposite

The progressive development of novel alloy and nanocomposite containing Pt NPs with multifunctional modalities could lead to better ways in PTT and RT [120]. Porous dendritic platinum–copper alloy nanoparticles (DPCN) as an imaging agent with high photothermal conversion efficiency and excellent photothermal stability have developed for cancer therapy [121]. DPCN loaded with doxorubicin (DPCN-Dox) could release the drugs in response to NIR light or moderate acidic stimulus. Cells internalized DPCN through clathrin-dependent endocytosis and micropinocytosis. Therefore, the internalized DPCN-Dox by PC-9 cancer cells under NIR irradiation revealed more efficient combined chemophotothermal (CPT) killing of cancer cells compared with the ones treated with DPCN plus NIR or Dox only. Upon the guidance of photoacoustic imaging, DPCN-mediated PTT could efficiently inhibit tumor growth *in vivo*. At the same time, DPCN- Dox completely suppressed the tumor growth even under a lower photothermal temperature (41.2 °C recorded at 12 h, and 42.1 °C at 24 h), compared with PTT (~45 °C) [121]. Therefore, hyperthermia adverse effects could be curbed by sparing normal tissues in combination therapy [121]. Wang et al. employed thermo-sensitive aspartate octapeptide-modified dendritic platinum-copper alloy nanoparticle (Asp-DPCN) which has a high affinity for binding to bone-formation, and bone resorption surface, respectively [122]. Glycine octapeptide-modified dendritic platinum-copper alloy nanoparticle (Gly-DPCN) was synthesized as a negative control. Dendritic platinum-copper alloy nanoparticles (DPCN) as an imaging agent exhibited great photothermal conversion efficiency, and high drug loading capacity [122]. Evaluation of the heating capability indicated that the temperature of Asp-DPCN absorbed hydroxyapatite tablet increased to 76 °C compared with that of 53 °C for Gly-DPCN. The *in vivo* bone targeting efficiencies of Asp-DPCN in mice models demonstrated that Asp-DPCN accumulated in bone tumors more efficiently than Gly-DPCN, resulting in the increased temperature to ~47 °C at 48 h for PTT. Finally, the tumor growth reduced efficiently by Asp-DPCN + NIR compared to monotherapy group Asp-DPCN or NIR. X-ray imaging was performed to examine the bone morphologic changes in tumors and, results showed the proximal tibias of mice groups treated with the PBS + NIR, Asp-DPCN, and Gly-DPCN + NIR were severely destructed, while the ones in the Asp-DPCN + NIR group were less destructed [122]. Li et al. have introduced the uniform nanoassembly of concave Pt Cu octopod nanoframes (OPCNs) modified with polyethylene glycol (PEG), and folic acid (FA) (OPCNs-PEG-FA) as a radio-sensitizer for combined PTT/RT against a tumor. The octopod OPCNs nanocrystals with a concave structure have exhibited eight symmetric feet with an average edge breadth of about 42.6 nm, and feet length of around 20.7 nm. The thermogenesis of the OPCNs-PEG-FA for tumor therapy revealed the rapid temperature increasing above 53 °C with nanoparticles concentration of 200 μg mL^{-1} after exposure to laser 808 nm for 5 min [123]. HepG2 cells internalized OPCNs-PEG-FA via clathrin-mediated, and caveolae-mediated endocytosis pathways were irradiated with NIR laser (808 nm, 2.4 W cm^{-2}, 5 min), and X-ray (120 kvp, 10 Gy, 10 min) individually or in conjunction. HepG2 cells treated with OPCNs-PEG-FA in combination with RT, and PTT, decreased the cell viability about 40% lower than that of OPCNs-PEG-FA mediated RT, and 20% lower compared with OPCNs-PEG-FA enhanced PTT [123]. X-ray (120 kvp, 10 Gy, 10 min), and NIR laser (808 nm, 2.4 W cm^{-2}, 5 min) irradiation in the presence of OPCNs-PEG-FA induced acute DNA damage which resulted in late-stage apoptosis subsequently [123]. The calculated combination index (CI) value for combination therapy was about 0.746, showed the synergistic effect of RT + PTT for applying OPCNs-PEG-FA nano assemblies [123]. Via *i.v.* injection of OPCNs-PEG-FA and NIR laser irradiation (808 nm), rapid increase up to 54.7 °C in heat generation at tumor region can intercept tumor cells. Whiles, the sideward tissue almost kept to physiological temperature [123]. Higher accumulation of OPCNs-PEG-FA in the tumor compared to bare OPCNs at 1 and 48 h after *i.v.* injection. Internalization of OPCNs-PEG-FA into tumor cells readily occurs via EPR effect and FA targeting. These nano assemblies caused tumor suppression by synergistic effect and also revealed no vivid systemic toxicity. So OPCNs-PEG-FA has been introduced as a biocompatible theranostic nanoassembly to treat cancer cells [123]. Deng et al. prepared multifoliate PEGylated PtRu bimetallic nano assemblies (PtRu-PEG BNCs) as multifunctional theranostic nano complexes for CT imaging, and a synergistic thermoradiotherapy [124]. PtRu-PEG BNCs with resembling Trifolium-like structures possessed superb photothermal conversion efficiency (44.5%) for its ability to switch absorbed NIR to heat. PtRu-PEG BNCs displayed outstanding CT signal increment, and a synergistic thermoradiotherapy because of the presence of platinum. The incubation of 4T1 cells with PtRu-PEG BNCs reduced the survival rate to 38.1% by the synergistic effect of PTT, and RT which could activate the cell apoptosis pathway. While individual RT, and hyperthermia cannot result in effective tumor cell apoptosis, the viability of 4T1 cells was about 79% (under laser irradiation), and 68% (under X-ray irradiation), respectively. The synergistic thermoradiotherapy *in vivo* by PtRu-PEG BNCs as the photothermal agents, and radiosensitizers demonstrated that the hyperthermia induced by PtRu-PEG BNCs under laser irradiation [124]. Pt atoms accelerated DNA degradation under irradiation of X-ray and also they could significantly inhibit the tumor volume. In therapy with PEG BNCs + NIR could partly restrain the tumor volume, and PEG BNCs + RT exhibited elevated tumor growth inhibition. These findings revealed that PtRu-PEG BNCs showed great potential for theranostic nanomedicine in CT imaging and a synergistic thermoradiotherapy [124]. Table 3 summarizes different platinum based nanostructure reported as PTT and RT agents applied on various types of tumor cells *in vitro* and *in vivo*.

2. Pathway to clinical trial

At present, dozens of iron and gold nanostructures have been approved by FDA for the treatment of various cancers, and some other metallic-based nanostructures were in clinical trials [125]. Among these nanostructures, PEG-coated silica-gold nanoshells (AuroLase), utilized for thermal ablation of tumors in response to near-infrared light, and polysiloxane Gd-chelates-based nanoparticles (AGuIX) used as a radiosensitizer in cancer radiotherapy [125].

Preclinical research of photothermal ablation of tumors in small animals utilizing nanoparticles will continue to grow quite quickly [126], but the speed of clinical translation is extremely slow, as very few of them are now under clinical trials. The first clinical trials of photothermal nanoparticles were performed on PEGylated silica-cored Au nanoshells appearing as AuroShell® particles in 2008 [127]. Thus AuroLase Therapy based on Au nanoshells permitted the precise thermal ablation of the tumor after using NIR (808 nm) laser light along its

Table 3
Summary of recent advancements of different platinum based nanostructures reported as PTT and RT and characteristics of testing (NP type, cells, and tumor).

Platinum based nanostructure						
Type	NPs size	Laser	η	RT	Therapeutically effect	*Ref.*
Platinum nanoparticles (PtNPs)	12.2 ± 0.7 nm	*in vitro*: (1.0 and 1.5 W cm^{-2}, 10 min, 808-nm)	(−)	6 mv, (2, 4, and 6 Gy), 200 cGy min^{-1}.	A noticeable decrement in cell viability of the C540 (B16/F10) cell line was observed in PTT/RT (1.5 W cm^{-2} laser radiation and 6 Gy X-ray radiation) incubated by 100 μg mL^{-1} PtNPs, compared to the other groups after 72 h incubation. Dual radiation of laser light and X-ray into PtNPs considerably improved the treatment via reactive oxygen species (ROS) production.	[27]
Worm-like platinum (Pt) nanoparticles (Pt nanoworms)	~100 nm	*in vitro:* (0.75 W. cm^{-2}, 10 min, 1064 nm); *in vivo:* (0.6 W. cm^{-2}, 10 min, 1064 nm)	38.9%	*in vitro*: (0, 2, 4, and 6 Gy); *in vivo*: 6 Gy	Pt nano worms in 4T1 breast cancer cells after exposure to 1064-nm caused laser-induced photothermal killing due to the necrocytosis by hyperthermia. The cell incubated with the Pt nano worms under the X-ray, demonstrated enhancing in radiotherapy effect; The tumor growth is completely inhibited by using mild photothermal therapy and radiotherapy due to the photothermally improved hypoxia and Pt increased X-ray absorption.	[112]
Mesoporous platinum nanostructure (Pt MN)	<11 nm	*in vitro:* (1 & 1.5 W cm^{-2}, 10 min, 808 nm)	(−)	(0, 2, 4, and 6 Gy)	Pt MN + PTT + RT led to a deep cell killing (~1%) in the C540 (B16/F10) due to the ROS production and heat generation.	[114]
Dendritic Platinum–Copper Alloy Nanoparticles (DPCN)	(−)	*in vitro:* (6.4 W. cm^{-2},5 min, 808 nm); *in vivo:* (0.75 & 1 W. cm^{-2}, 10 min, 808 nm)	(−)	(−)	PC-9 cancer cells internalized DPCN through clathrin-dependent endocytosis and micropinocytosis. It revealed more efficient combined chemophotothermal (CPT) killing of cancer cells under NIR irradiation; Upon photoacoustic imaging guidance, DPCN-mediated photothermal treatment could efficiently inhibit tumor growth *in vivo*.	[121]
Aspartate octapeptide-modified dendritic platinum-copper alloy nanoparticle (Asp-DPCN)	~300 nm	*in vitro:* (3.6 W. cm^{-2}, 5 min, 808 nm); *in vivo:* (3.6 W. cm^{-2}, 10 min, 808 nm)	37.51%	(−)	Asp-DPCN with higher affinities toward bone fragments accumulated more efficiently around bone tumors and increased temperature in bone tumors during PTT. Therefore, Asp-DPCN efficiently depressed the tumor growth but also significantly reduced the osteoclastic bone destruction.	[122]
Octopod platinum-copper nanoframes (OPCNs) modified with polyethylene glycol (PEG) and folic acid (FA) (OPCNs-PEG-FA)	edge breadth ~42.6 nm/feet length of 20.7 nm,	*in vitro & in vivo:* (2.4 mW. cm^{-2}, 5 min, 808 nm)	(−)	*in vitro & in vivo:* (120 kvp, 10 Gy, 10 min)	The OPCNs-PEG-FA with strong NIR absorption and X-ray radio-sensitization, exhibited remarkable PTT and RT synergistic effect on HepG2 cell viability and caused great tumor growth inhibition when treated with NIR laser and X-ray.	[123]
PEGylated PtRu bimetallic nanocomplexes (PtRu-PEG BNCs)	20 nm	*in vitro & in vivo*: (0.75 mW. cm^{-2}, 5 min, 808 nm)	44.5%	*in vitro:* 6 Gy & *in vivo*: 4 Gy	Cell viability of 4T1 cells incubated with PtRu-PEG BNCs exposed to NIR laser and X-ray greatly reduced to 38.1% via induction of apoptosis. The volume of the tumor in mice subjected to PtRu-PEG BNCs + NIR + RT, was significantly inhibited.	[124]

Abbreviations: NIR, near-infrared; NP, nanoparticle; Ns, nanostructure; PTT, photothermal therapy; RT, radiotherapy.

irregular boundaries while keeping healthy the surrounding tissue [128].

An efficacy of AuroLase Therapy (Nanospectra Biosciences, Inc., Houston, TX) was studied in patients with primary and/or metastatic lung tumors (https://clinicaltrials.gov/Identifier: NCT01679470) in the United States. Patients were treated with systemic *i.v.* infusion of Au nanoshells and then escalating dose of laser radiation delivered by optical fiber via bronchoscopy. In the second clinical trial targeted Au nanoshells were examined with focusing on treatment of patients with refractory and/or recurrent tumors of the head and neck (https://clinicaltrials.gov/Identifier: NCT00848042). Potentially targeted Au nanoshells could improve their accumulation in tumors as evidenced by the successful vascular-targeted PTT of glioma in mice [129], so far in these two clinical trials is expected that Au nanoshells purely accumulated in patients based on the EPR effect. AuroLase Therapy relies on laser excitation of gold-silica nanoshells (GSNs) is utilized for selectively targeting and treating focal lesions within the prostate [130]. Healthy tissue experiences mild and reversible hyperthermia at lower concentrations of GSN, while the higher concentrations of GSN within the cancerous lesion generate sufficient photothermal energy to produce coagulative necrosis [130]. AGuIX nanoparticles have recently been approved for clinical trials for multiple metastatic brain tumors [131]. AGuIX nanoparticles as radiosensitizers with a diameter of 3 ± 1.5 nm cause an increase in irradiation effect by a factor of 1.1–2.5 depending on the energy of the photon beam. The radiosensitizing effect was observed in the kilo electron volt region (220 kVp) as well as in the mega electron volt (6 MV) region on various cancer cell lines including pancreatic cancer, glioblastoma cells, head and neck squamous cell carcinoma, cervical cell carcinoma, and prostate cancer cells. Also, for obtaining the radiosensitizing effect of AGuIX a wide range of animal models including mouse melanoma brain metastasis model, rat glioblastoma model, and orthotopic mouse models of non-small cell lung carcinoma, mouse models of head and neck cancer, the mouse model of liver cancer, and a rat model of chondrosarcoma were used. AGuIX as a promising type of MRI-guided radiotherapy agent showed accumulation in the tumor area and elimination by the renal route in animal model systems [132].

There is a long way for pushing photothermal nanoparticles from the bench to the bedside. The selection of the best metallic nanostructures requires great attention. It is very difficult to obtain FDA approval for nanostructures containing heavy metal elements which cannot be degraded *in vivo* and their long-term toxicity concerns. In addition, another leading problem is the large-scale production of most nanoparticles which lose their uniformity and reproducibility. Therefore,

great efforts are needed to ensure the high-quality control (e.g., good laboratory practice and good manufacturing practice) of nanoparticles that are to be translated. Finally, a closer partnership among academic researchers, clinicians, pharmaceutical industries, the National Cancer Institute, and the FDA is necessary to promote the translational research of promising photothermal nanoparticles.

3. Conclusion and outlook

In this review, we highlighted the recent advances in PTT and RT based on metal nanostructures for cancer therapy. *In vitro*, and *in vivo* studies were performed on the effects of each nanostructure in order to compare, and optimize the medical efficiencies in biological conditions. The combination of PTT and RT has exhibited synergistic anticancer efficacy in a "1 + 1>2" manner. Indeed, photothermal agents upon special NIR laser irradiation in the cancer tissue induce hyperthermia and eliminate cancer cells. Also, they act as a heat trigger to promote oxygen level in the tumor area and simplify cells to elevate RT. Optimized RT together with PTT could assist to ablate tumors, especially tumors in depth. Synergistic PTT/RT has exhibited supreme proficiency in vanquishing radioresistance cancers. Contrary to the extensive development, and promising potential of nanomaterials for PTT, and RT, some certain issues require to be considered. The photothermal conversion performance will considerably be affected by the dosage of photothermal agents, and NIR light intensity/irradiation time for effective heat generation, varies among different nanomaterials mentioned in this review. The photothermal conversion performance of some kinds of nanomaterials has been presented in a text. It requires more attempts to develop novel nanomaterials with desirable photothermal conversion, and radiosensitization performance to get satisfactory PTT, and RT consequence, and decrease the administered dose of nanomaterials. Despite the deeper penetration of NIR laser in tumor tissues, the penetrated depth is restricted. Thus, non-invasive PTT is considered a frequent approach for superficial tumors. Effective combined PTT and RT can be accompanied by minimal intervention via the design of novel non-invasive medical devices. Shortcomings of the long-term cytotoxicity of these nanomaterials, especially those with poor biodegradability remains unclear and merits more regard in future investigations. In this way, Photothermal, and radiosensitizer-based nanomaterials reveal more desirable efficiency in biodegradability and biocompatibility. It could result in the excellent anticancer efficacy of some metals in a lower dosage with the favor of hyperthermia and RT. The systematic administration may cause undesired side effects. Therefore, low price nanomaterials with surface modification via targeting moieties on their surface can promote intracellular accumulation by particular nano-cell interactions in tumor sites with improving PTT, and RT efficiency, and decreasing side effects. Finally, the synergistic effect mechanism for combined PTT and RT will require more extensive research. Hyperthermia enhances blood flow, vascular permeability, and oxygenation within tumor tissues, subsequently enhancing the RT therapeutic outcome of combined therapy. RT resistance is one of the most important hindrances against effective cancer therapy. But PTT remarkably diminishes the resistance via lowering the RT dosage. Molecular mechanisms of RT and PTT still require to be explored. Surely, investigations on tumor biology will assist us to achieve a better understanding of the intrinsic mechanism for RT resistance, comforting the design of novel nanoplatforms for efficient cancer therapies. Despite the existing challenges, the combination of PTT and RT may open new avenues for cancer therapy based on existing papers.

Author contributions

N. Sattarahmady designed and supervised the review. All the authors wrote the original draft and reviewed the final manuscript.

Additional information competing interests

The authors declare that they have no competing interests.

Acknowledgments

We would like to thank the Research Council of Shiraz University of Medical Sciences (18516) for supporting this research.

References

[1] S.O. Freytag, K.R. Rogulski, D.L. Paielli, J.D. Gilbert, J.H. Kim, A novel three-pronged approach to kill cancer cells selectively: concomitant viral, double suicide gene, and radiotherapy, J Hum Gene Ther 9 (9) (1998) 1323–1333.
[2] P.J. Hesketh, D. Batchelor, M. Golant, G.H. Lyman, N. Rhodes, D. Yardley, Chemotherapy-induced alopecia: psychosocial impact and therapeutic approaches, J Support Care Cancer 12 (8) (2004) 543–549.
[3] T.R. Tritton, J. Hickman, How to kill cancer cells: membranes and cell signaling as targets in cancer chemotherapy, *J Cancer cells* (Cold Spring Harbor, NY: 1989) 2 (4) (1990) 95.
[4] M.J. Zelefsky, D.H. Kraus, D.G. Pfister, A. Raben, J.P. Shah, E.W. Strong, et al., Combined chemotherapy and radiotherapy versus surgery and postoperative radiotherapy for advanced hypopharyngeal cancer, J Head Neck-J Sci Spec 18 (5) (1996) 405–411.
[5] C. Holohan, S. Van Schaeybroeck, D.B. Longley, P.G. Johnston, Cancer drug resistance: an evolving paradigm, J Nat Rev Cancer 13 (10) (2013) 714–726.
[6] M. Mallory, E. Gogineni, G.C. Jones, L. Greer, C.B. Simone II, Therapeutic hyperthermia: the old, the new, and the upcoming, J Crit Rev Oncol Hemat 97 (2016) 56–64.
[7] M. Falk, R. Issels, Hyperthermia in oncology, Int. J. Hyperther. 17 (1) (2001) 1–18.
[8] P. Wust, B. Hildebrandt, G. Sreenivasa, B. Rau, J. Gellermann, H. Riess, et al., Hyperthermia in combined treatment of cancer, J lancet Oncol 3 (8) (2002) 487–497.
[9] V. Shanmugam, S. Selvakumar, C.-S. Yeh, Near-infrared light-responsive nanomaterials in cancer therapeutics, J Chem Soc Rev 43 (17) (2014) 6254–6287.
[10] I. Postiglione, A. Chiaviello, G. Palumbo, Enhancing photodynamyc therapy efficacy by combination therapy: dated, current and oncoming strategies, J. Canc. 3 (2) (2011) 2597–2629.
[11] C. Zhang, L. Yan, Z. Gu, Y. Zhao, Strategies based on metal-based nanoparticles for hypoxic-tumor radiotherapy, J. Chem. Sci. 10 (29) (2019) 6932–6943.
[12] D. Kwatra, A. Venugopal, S. Anant, Nanoparticles in radiation therapy: a summary of various approaches to enhance radiosensitization in cancer, Transl. Cancer Res. 2 (4) (2013) 330–342.
[13] J. Li, W. Shang, Y. Li, S. Fu, J. Tian, L. Lu, Advanced nanomaterials targeting hypoxia to enhance radiotherapy, Int. J. Nanomed. 13 (2018) 5925.
[14] N. Behzadpour, N. Akbari, N. Sattarahmady, Photothermal inactivation of methicillin-resistant Staphylococcus aureus: anti-biofilm mediated by a polypyrrole–carbon nanocomposite, IET Nanobiotechnol. 13 (8) (2019) 800–807.
[15] N. Behzadpour, N. Sattarahmady, N. Akbari, Antimicrobial photothermal treatment of pseudomonas aeruginosa by a carbon nanoparticles-polypyrrole nanocomposite, J Biomed Phys Eng 9 (6) (2019) 661.
[16] G. Tondro, N. Behzadpour, Z. Keykhaee, N. Akbari, N. Sattarahmady, Carbon@ polypyrrole nanotubes as a photosensitizer in laser phototherapy of pseudomonas aeruginosa, Colloids Surf. B Biointerfaces 180 (2019) 481–486.
[17] N. Behzadpour, A. Ranjbar, N. Azarpira, N. Sattarahmady, Development of a composite of polypyrrole-coated carbon nanotubes as a sonosensitizer for treatment of melanoma cancer under multi-Step ultrasound irradiation, Ultrasound Med. Biol. 46 (9) (2020) 2322–2334.
[18] K. Ghanbari, M. Mousavi, M. Shamsipur, M. Rahmanifar, H. Heli, Change in morphology of polyaniline/graphite composite: a fractal dimension approach, Synth. Met. 156 (14–15) (2006) 911–916.
[19] H. Heli, A. Rahi, Synthesis and applications of nanoflowers, Recent Pat Nanotech 10 (2) (2016) 86–115.
[20] M. Gorgizadeh, N. Behzadpour, F. Salehi, F. Daneshvar, R.D. Vais, R. Nazari-Vanani, et al., A MnFe2O4/C nanocomposite as a novel theranostic agent in MRI, sonodynamic therapy and photothermal therapy of a melanoma cancer model, J. Alloys Compd. 816 (2020) 152597.
[21] E. Soratijahromi, S. Mohammadi, R.D. Vais, N. Azarpira, N. Sattarahmady, Photothermal/sonodynamic therapy of melanoma tumor by a gold/manganese dioxide nanocomposite: *In vitro* and *in vivo* studies, Photodiagnosis Photodyn. Ther. 31 (2020) 101846.
[22] S.M. Mortazavi, M. Khatami, I. Sharifi, H. Heli, K. Kaykavousi, M.H.S. Poor, et al., Bacterial biosynthesis of gold nanoparticles using Salmonella enterica subsp. enterica serovar Typhi isolated from blood and stool specimens of patients, J. Cluster Sci. 28 (5) (2017) 2997–3007.
[23] L.A. Austin, M.A. Mackey, E.C. Dreaden, M.A. El-Sayed, The optical, photothermal, and facile surface chemical properties of gold and silver nanoparticles in biodiagnostics, therapy, and drug delivery, Arch. Toxicol. 88 (7) (2014) 1391–1417.

[24] M. Khatami, S.M. Mortazavi, Z. Kishani-Farahani, A. Amini, E. Amini, H. Heli, Biosynthesis of silver nanoparticles using pine pollen and evaluation of the antifungal efficiency, Iran. J. Biotechnol. 15 (2) (2017) 95.
[25] P. Huang, L. Bao, C. Zhang, J. Lin, T. Luo, D. Yang, et al., Folic acid-conjugated silica-modified gold nanorods for X-ray/CT imaging-guided dual-mode radiation and photo-thermal therapy, Biomaterials 32 (36) (2011) 9796–9809.
[26] X. Yi, K. Yang, C. Liang, X. Zhong, P. Ning, G. Song, et al., Imaging-guided combined photothermal and radiotherapy to treat subcutaneous and metastatic tumors using iodine-131-doped copper sulfide nanoparticles, Adv. Funct. Mater. 25 (29) (2015) 4689–4699.
[27] F. Daneshvar, F. Salehi, M. Karimi, R.D. Vais, M. Mosleh-Shirazi, N. Sattarahmady, Combined X-ray radiotherapy and laser photothermal therapy of melanoma cancer cells using dual-sensitization of platinum nanoparticles, J. Photochem. Photobiol. B Biol. 203 (2020) 111737.
[28] M. Gorgizadeh, N. Azarpira, N. Sattarahmady, *In vitro* and in vivo tumor annihilation by near-infrared photothermal effect of a NiFe2O4/C nanocomposite, Colloids Surf. B Biointerfaces 170 (2018) 393–400. 29.
[29] A.D. Paro, I. Shanmugam, A.L. van de Ven, Nanoparticle-mediated x-ray radiation enhancement for cancer therapy, Methods Mol. Biol. 1530 (2017) 391–401.
[30] M.A. García, Surface plasmons in metallic nanoparticles: fundamentals and applications, J Phys D 44 (28) (2011) 283001.
[31] M. Li, S.K. Cushing, N. Wu, Plasmon-enhanced optical sensors: a review, Analyst 140 (2) (2015) 386–406.
[32] J. Chen, C. Ning, Z. Zhou, P. Yu, Y. Zhu, G. Tan, et al., Nanomaterials as photothermal therapeutic agents, Prog. Mater. Sci. 99 (2019) 1–26.
[33] S.Y. Fam, C.F. Chee, C.Y. Yong, K.L. Ho, A.R. Mariatulqabtiah, W.S. Tan, Stealth coating of nanoparticles in drug-delivery systems, Nanomaterials 10 (4) (2020) 787.
[34] Z. Kayani, O. Firuzi, A.-K. Bordbar, Doughnut-shaped bovine serum albumin nanoparticles loaded with doxorubicin for overcoming multidrug-resistant in cancer cells, Int. J. Biol. Macromol. 107 (2018) 1835–1843.
[35] Z. Kayani, A.-K. Bordbar, O. Firuzi, Novel folic acid-conjugated doxorubicin loaded β-lactoglobulin nanoparticles induce apoptosis in breast cancer cells, Biomed. Pharmacother. 107 (2018) 945–956.
[36] X.-Y. Su, P.-D. Liu, H. Wu, N. Gu, Enhancement of radiosensitization by metal-based nanoparticles in cancer radiation therapy, Cancer Biol Med 11 (2) (2014) 86.
[37] S. Medici, M. Peana, V.M. Nurchi, J.I. Lachowicz, G. Crisponi, M.A. Zoroddu, Noble metals in medicine: latest advances, Coord. Chem. Rev. 284 (2015) 329–350.
[38] J.-J. Hu, Y.-J. Cheng, X.-Z. Zhang, Recent advances in nanomaterials for enhanced photothermal therapy of tumors, Nanoscale 10 (48) (2018) 22657–22672.
[39] M. Chhowalla, H.S. Shin, G. Eda, L.-J. Li, K.P. Loh, H. Zhang, The chemistry of two-dimensional layered transition metal dichalcogenide nanosheets, Nat. Chem. 5 (4) (2013) 263–275.
[40] Q. Wang, J. Lai, D. Sun, Review of photo response in semiconductor transition metal dichalcogenides based photosensitive devices, Opt. Mater. Express 6 (7) (2016) 2313–2327.
[41] S. Zhu, L. Gong, J. Xie, Z. Gu, Y. Zhao, Design, synthesis, and surface modification of materials based on transition-metal dichalcogenides for biomedical applications, Small Methods 1 (12) (2017) 1700220.
[42] C. Zhong, X. Zhao, L. Wang, Y. Li, Y. Zhao, Facile synthesis of biocompatible MoSe 2 nanoparticles for efficient targeted photothermal therapy of human lung cancer, RSC Adv. 7 (12) (2017) 7382–7391.
[43] M. Ma, Y. Huang, H. Chen, X. Jia, S. Wang, Z. Wang, et al., Bi2S3-embedded mesoporous silica nanoparticles for efficient drug delivery and interstitial radiotherapy sensitization, Biomaterials 37 (2015) 447–455.
[44] J. Liu, X. Zheng, L. Yan, L. Zhou, G. Tian, W. Yin, et al., Bismuth sulfide nanorods as a precision nanomedicine for *in vivo* multimodal imaging-guided photothermal therapy of tumor, ACS Nano 9 (1) (2015) 696–707.
[45] J. Li, F. Jiang, B. Yang, X.-R. Song, Y. Liu, H.-H. Yang, et al., Topological insulator bismuth selenide as a theranostic platform for simultaneous cancer imaging and therapy, Sci. Rep. 3 (1) (2013) 1–7.
[46] Y. Wang, S. Song, T. Lu, Y. Cheng, Y. Song, S. Wang, et al., Oxygen-supplementing mesoporous polydopamine nanosponges with WS2 QDs-embedded for CT/MSOT/MR imaging and thermoradiotherapy of hypoxic cancer, Biomaterials 220 (2019) 119405.
[47] W. Jiang, Q. Li, L. Xiao, J. Dou, Y. Liu, W. Yu, et al., Hierarchical multiplexing nanodroplets for imaging-guided cancer radiotherapy via DNA damage enhancement and concomitant DNA repair prevention, ACS Nano 12 (6) (2018) 5684–5698.
[48] D. Huo, S. Liu, C. Zhang, J. He, Z. Zhou, H. Zhang, et al., Hypoxia-targeting, tumor microenvironment responsive nanocluster bomb for radical-enhanced radiotherapy, ACS Nano 11 (10) (2017) 10159–10174.
[49] Y. Yong, X. Cheng, T. Bao, M. Zu, L. Yan, W. Yin, et al., Tungsten sulfide quantum dots as multifunctional nanotheranostics for *in vivo* dual-modal image-guided photothermal/radiotherapy synergistic therapy, ACS Nano 9 (12) (2015) 12451–12463.
[50] F. Qi, R. Liu, Tumor-targeted and biocompatible MoSe 2 nanodots@ albumin nanospheres as a dual-modality therapy agent for synergistic photothermal radiotherapy, Nanoscale Res Lett 14 (1) (2019) 67.
[51] S. Siva, P. Lobachevsky, M.P. MacManus, T. Kron, A. Möller, R.J. Lobb, et al., Radiotherapy for non–small cell lung cancer induces DNA damage response in both irradiated and out-of-field normal tissues, Clin. Canc. Res. 22 (19) (2016) 4817–4826.
[52] M. Goldstein, M.B. Kastan, The DNA damage response: implications for tumor responses to radiation and chemotherapy, Annu. Rev. Med. 66 (2015) 129–143.
[53] S. Shen, Y. Chao, Z. Dong, G. Wang, X. Yi, G. Song, et al., Bottom-up preparation of uniform ultrathin rhenium disulfide nanosheets for image-guided photothermal radiotherapy, Adv. Funct. Mater. 27 (28) (2017) 1700250.
[54] J. Fang, H. Nakamura, H. Maeda, The EPR effect: unique features of tumor blood vessels for drug delivery, factors involved, and limitations and augmentation of the effect, Adv. Drug Deliv. Rev. 63 (3) (2011) 136–151.
[55] D.R. Grimes, P. Kannan, A. McIntyre, A. Kavanagh, A. Siddiky, S. Wigfield, et al., The role of oxygen in avascular tumor growth, PloS One 11 (4) (2016), e0153692.
[56] C. Cao, J. Zhang, C. Yang, L. Xiang, W. Liu, Albumin exfoliated titanium disulfide nanosheet: a multifunctional nanoplatform for synergistic photothermal/radiation colon cancer therapy, OncoTargets Ther. 12 (2019) 6337.
[57] P. Vijayaraghavan, C.H. Liu, R. Vankayala, C.S. Chiang, K.C. Hwang, Designing multi-branched gold nanoechinus for NIR light activated dual modal photodynamic and photothermal therapy in the second biological window, Adv. Mater. 26 (39) (2014) 6689–6695.
[58] A.L. Antaris, H. Chen, K. Cheng, Y. Sun, G. Hong, C. Qu, et al., A small-molecule dye for NIR-II imaging, Nat. Mater. 15 (2) (2016) 235–242.
[59] W. Yin, T. Bao, X. Zhang, Q. Gao, J. Yu, X. Dong, L. Yan, Z. Gu, Y. Zhao, Biodegradable MoO_x nanoparticles with efficient near-infrared photothermal and photodynamic synergetic cancer therapy at the second biological window, Nanoscale 10 (3) (2018) 1517–1531.
[60] B. Guo, Z. Sheng, D. Hu, C. Liu, H. Zheng, B. Liu, Through scalp and skull NIR-II photothermal therapy of deep orthotopic brain tumors with precise photoacoustic imaging guidance, Adv. Mater. 30 (35) (2018) 1802591.
[61] W. Tang, Z. Dong, R. Zhang, X. Yi, K. Yang, M. Jin, et al., Multifunctional two-dimensional core–shell mxene@ gold nanocomposites for enhanced photo–radio combined therapy in the second biological window, ACS Nano 13 (1) (2018) 284–294.
[62] E. Boisselier, D. Astruc, Gold nanoparticles in nanomedicine: preparations, imaging, diagnostics, therapies and toxicity, Chem. Soc. Rev. 38 (6) (2009) 1759–1782.
[63] W.-S. Cho, M. Cho, J. Jeong, M. Choi, H.-Y. Cho, B.S. Han, et al., Acute toxicity and pharmacokinetics of 13 nm-sized PEG-coated gold nanoparticles, Toxicol. Appl. Pharmacol. 236 (1) (2009) 16–24.
[64] E.E. Connor, J. Mwamuka, A. Gole, C.J. Murphy, M.D. Wyatt, Gold nanoparticles are taken up by human cells but do not cause acute cytotoxicity, Small 1 (3) (2005) 325–327.
[65] T. Mironava, M. Hadjiargyrou, M. Simon, V. Jurukovski, M.H. Rafailovich, Gold nanoparticles cellular toxicity and recovery: effect of size, concentration and exposure time, Nanotoxicology 4 (1) (2010) 120–137.
[66] X. Huang, P.K. Jain, I.H. El-Sayed, M.A. El-Sayed, Gold nanoparticles: interesting optical properties and recent applications in cancer diagnostics and therapy, Nanomedicine 2 (5) (2007) 681–693.
[67] G. Qiao, L. Zhuo, Y. Gao, L. Yu, N. Li, B. Tang, A tumor mRNA-dependent gold nanoparticle–molecular beacon carrier for controlled drug release and intracellular imaging, Chem. Commun. (J. Chem. Soc. Sect. D) 47 (26) (2011) 7458–7460.
[68] N. Sattarahmady, Z. Kayani, H. Heli, Highly simple and visual colorimetric detection of Brucella melitensis genomic DNA in clinical samples based on gold nanoparticles, J. Iran. Chem. Soc. 12 (9) (2015) 1569–1576.
[69] M. Negahdary, M. Behjati-Ardakani, N. Sattarahmady, H. Yadegari, H. Heli, Electrochemical aptasensing of human cardiac troponin I based on an array of gold nanodumbbells-Applied to early detection of myocardial infarction, Sensor. Actuator. B Chem. 252 (2017) 62–71.
[70] D. Pissuwan, T. Niidome, M.B. Cortie, The forthcoming applications of gold nanoparticles in drug and gene delivery systems, J. Contr. Release 149 (1) (2011) 65–71.
[71] J.-L. Li, M. Gu, Gold-nanoparticle-enhanced cancer photothermal therapy, IEEE J. Sel. Top. Quant. Electron. 16 (4) (2009) 989–996.
[72] J.F. Hainfeld, L. Lin, D.N. Slatkin, F.A. Dilmanian, T.M. Vadas, H.M. Smilowitz, Gold nanoparticle hyperthermia reduces radiotherapy dose, Nanomed-Nanotechnol 10 (8) (2014) 1609–1617.
[73] F. Rahimi-Moghaddam, N. Azarpira, N. Sattarahmady, Evaluation of a nanocomposite of PEG-curcumin-gold nanoparticles as a near-infrared photothermal agent: an *in vitro* and animal model investigation, Laser Med. Sci. 33 (8) (2018) 1769–1779.
[74] M. Heidari, N. Sattarahmady, N. Azarpira, H. Heli, A. Mehdizadeh, T. Zare, Photothermal cancer therapy by gold-ferrite nanocomposite and near-infrared laser in animal model, Laser Med. Sci. 31 (2) (2016) 221–227.
[75] W.H. De Jong, W.I. Hagens, P. Krystek, M.C. Burger, A.J. Sips, R.E. Geertsma, Particle size-dependent organ distribution of gold nanoparticles after intravenous administration, Biomaterials 29 (12) (2008) 1912–1919.
[76] X.D. Zhang, Z. Luo, J. Chen, X. Shen, S. Song, Y. Sun, et al., Ultrasmall Au10− 12 (SG) 10− 12 nanomolecules for high tumor specificity and cancer radiotherapy, Adv. Mater. 26 (26) (2014) 4565–4568.
[77] X.-D. Zhang, Z. Luo, J. Chen, S. Song, X. Yuan, X. Shen, et al., Ultrasmall glutathione-protected gold nanoclusters as next generation radiotherapy sensitizers with high tumor uptake and high renal clearance, Sci. Rep. 5 (2015) 8669.
[78] K. Rahme, M.T. Nolan, T. Doody, G.P. McGlacken, M.A. Morris, C. O'Driscoll, et al., Highly stable PEGylated gold nanoparticles in water: applications in biology and catalysis, RSC Adv. 3 (43) (2013) 21016–21024.
[79] L. Sandiford, A. Phinikaridou, A. Protti, L.K. Meszaros, X. Cui, Y. Yan, et al., Bisphosphonate-anchored PEGylation and radiolabeling of superparamagnetic

iron oxide: long-circulating nanoparticles for *in vivo* multimodal (T1 MRI-SPECT) imaging, ACS Nano 7 (1) (2013) 500–512.
[80] B.D. Chithrani, W.C. Chan, Elucidating the mechanism of cellular uptake and removal of protein-coated gold nanoparticles of different sizes and shapes, Nano Lett. 7 (6) (2007) 1542–1550.
[81] Y. Liu, H. Yuan, A.M. Fales, J.K. Register, T. Vo-Dinh, Multifunctional gold nanostars for molecular imaging and cancer therapy, Front Chem 3 (2015) 51.
[82] L. Tian, M. Fei, S. Tadepalli, J.J. Morrissey, E.D. Kharasch, S. Singamaneni, Bio-enabled gold superstructures with built-in and accessible electromagnetic hotspots, Adv Healthc Mater 4 (10) (2015) 1502–1509.
[83] N. Ma, Y.-W. Jiang, X. Zhang, H. Wu, J.N. Myers, P. Liu, et al., Enhanced radiosensitization of gold nanospikes via hyperthermia in combined cancer radiation and photothermal therapy, ACS Appl. Mater. Interfaces 8 (42) (2016) 28480–28494.
[84] X. Liu, X. Zhang, M. Zhu, G. Lin, J. Liu, Z. Zhou, et al., PEGylated Au@ Pt nanodendrites as novel theranostic agents for computed tomography imaging and photothermal/radiation synergistic therapy, ACS Appl. Mater. Interfaces 9 (1) (2017) 279–285.
[85] A.M. Bugaj, Targeted photodynamic therapy–a promising strategy of tumor treatment, Photochem. Photobiol. Sci. 10 (7) (2011) 1097–1109.
[86] X. Huang, P.K. Jain, I.H. El-Sayed, M.A. El-Sayed, Plasmonic photothermal therapy (PPTT) using gold nanoparticles, Laser Med. Sci. 23 (3) (2008) 217.
[87] V. Hosseini, M. Mirrahimi, A. Shakeri-Zadeh, F. Koosha, B. Ghalandari, S. Maleki, et al., Multimodal cancer cell therapy using Au@ Fe2O3 core–shell nanoparticles in combination with photo-thermo-radiotherapy, Photodiagnosis Photodyn. Ther. 24 (2018) 129–135.
[88] A. Neshastehriz, M. Tabei, S. Maleki, S. Eynali, A. Shakeri-Zadeh, Photothermal therapy using folate conjugated gold nanoparticles enhances the effects of 6 MV X-ray on mouth epidermal carcinoma cells, *J. Photochem. Photobiol.*, B 172 (2017) 52–60.
[89] T. Wolfe, D. Chatterjee, J. Lee, J.D. Grant, S. Bhattarai, R. Tailor, et al., Targeted gold nanoparticles enhance sensitization of prostate tumors to megavoltage radiation therapy *in vivo*, Nanomedicine 11 (5) (2015) 1277–1283.
[90] A.K. Parchur, G. Sharma, J.M. Jagtap, V.R. Gogineni, P.S. LaViolette, M.J. Flister, et al., Vascular interventional radiology-guided photothermal therapy of colorectal cancer liver metastasis with theranostic gold nanorods, ACS Nano 12 (7) (2018) 6597–6611.
[91] J. Keyvan Rad, A.R. Mahdavian, S. Khoei, S. Shirvalilou, Enhanced photogeneration of reactive oxygen species and targeted photothermal therapy of C6 glioma brain cancer cells by folate-conjugated gold–photoactive polymer nanoparticles, ACS Appl. Mater. Interfaces 10 (23) (2018) 19483–19493.
[92] A. González-Ruíz, G. Ferro-Flores, N. Jiménez-Mancilla, A. Escudero-Castellanos, B. Ocampo-García, M. Luna-Gutiérrez, et al., *In vitro* and *in vivo* synergistic effect of radiotherapy and plasmonic photothermal therapy on the viability of cancer cells using 177 Lu–Au-NLS-RGD-Aptamer nanoparticles under laser irradiation, J. Radioanal. Nucl. Chem. 318 (3) (2018) 1913–1921.
[93] X.-D. Li, Z. Wang, X.-R. Wang, D. Shao, X. Zhang, L. Li, et al., Berberine-loaded Janus gold mesoporous silica nanocarriers for chemo/radio/photothermal therapy of liver cancer and radiation-induced injury inhibition, Int J Nanotechnol Nanomed 14 (2019) 3967.
[94] W. Zhang, X. Ding, H. Cheng, C. Yin, J. Yan, Z. Mou, et al., Dual-targeted gold nanoprism for recognition of early apoptosis, dual-model imaging and precise cancer photothermal therapy, Theranostics 9 (19) (2019) 5610.
[95] R.N. Bose, L. Maurmann, R.J. Mishur, L. Yasui, S. Gupta, W.S. Grayburn, et al., Non-DNA-binding platinum anticancer agents: cytotoxic activities of platinum–phosphato complexes towards human ovarian cancer cells, Proc. Natl. Acad. Sci. Unit. States Am. 105 (47) (2008) 18314–18319.
[96] M. Galanski, M.A. Jakupec, B.K. Keppler, Update of the preclinical situation of anticancer platinum complexes: novel design strategies and innovative analytical approaches, Curr. Med. Chem. 12 (18) (2005) 2075–2094.
[97] Q. Cao, Y. Li, E. Freisinger, P.Z. Qin, R.K. Sigel, Z.-W. Mao, G-quadruplex DNA targeted metal complexes acting as potential anticancer drugs, Inorg Chem Front 4 (1) (2017) 10–32.
[98] J. Kim, M. Takahashi, T. Shimizu, T. Shirasawa, M. Kajita, A. Kanayama, et al., Effects of a potent antioxidant, platinum nanoparticle, on the lifespan of Caenorhabditis elegans, Mech. Ageing Dev. 129 (6) (2008) 322–331.
[99] E. Porcel, S. Liehn, H. Remita, N. Usami, K. Kobayashi, Y. Furusawa, et al., Platinum nanoparticles: a promising material for future cancer therapy? Nanotechnology 21 (8) (2010), 085103.
[100] A. Stepanov, A. Golubev, S. Nikitin, Y. Osin, A review on the fabrication and properties of platinum nanoparticles, Rev. Adv. Mater. Sci. 38 (2) (2014) 160–175.
[101] Z. Yazdani, H. Yadegari, H. Heli, A molecularly imprinted electrochemical nanobiosensor for prostate specific antigen determination, Anal. Biochem. 566 (2019) 116–125.
[102] M. Negahdary, H. Heli, Applications of nanoflowers in biomedicine, Recent Pat Nanotechnol 12 (1) (2018) 22–33.
[103] M. Negahdary, H. Heli, An ultrasensitive electrochemical aptasensor for early diagnosis of Alzheimer's disease, using a fern leaves-like gold nanostructure, Talanta 198 (2019) 510–517.
[104] M. Negahdary, M. Behjati-Ardakani, H. Heli, An electrochemical troponin T aptasensor based on the use of a macroporous gold nanostructure, Microchimica Acta 186 (6) (2019) 377.
[105] M. Negahdary, H. Heli, An electrochemical peptide-based biosensor for the Alzheimer biomarker amyloid-β (1–42) using a microporous gold nanostructure, Microchimica Acta 186 (12) (2019) 766.
[106] A. Medhat, S. Mansour, S. El-Sonbaty, E. Kandil, M. Mahmoud, Evaluation of the antitumor activity of platinum nanoparticles in the treatment of hepatocellular carcinoma induced in rats, Tumour Biol 39 (7) (2017), 1010428317717259.
[107] M.A. Ka, R. Ab Rashid, R.M. Lazim, N. Dollah, K.A. Razak, W. Rahman, Evaluation of radiosensitization effects by platinum nanodendrites for 6 MV photon beam radiotherapy, Radiat Phys Chem Oxf Engl 150 (2018) 40–45.
[108] P. Puja, P. Kumar, A perspective on biogenic synthesis of platinum nanoparticles and their biomedical applications, Spectrochim. Acta Mol. Biomol. Spectrosc. 211 (2019) 94–99.
[109] M. Manikandan, N. Hasan, H.-F. Wu, Platinum nanoparticles for the photothermal treatment of Neuro 2A cancer cells, Biomaterials 34 (23) (2013) 5833–5842.
[110] L. Ono, B. Yuan, H. Heinrich, B.R. Cuenya, Formation and thermal stability of platinum oxides on size-selected platinum nanoparticles: support effects, J. Phys. Chem. C 114 (50) (2010) 22119–22133.
[111] N.V. Long, N.D. Chien, T. Hayakawa, T. Matsubara, M. Ohtaki, M. Nogami, Sharp cubic and octahedral morphologies of poly (vinylpyrrolidone)-stabilised platinum nanoparticles by polyol method in ethylene glycol: their nucleation, growth and formation mechanisms, J. Exp. Nanosci. 7 (2) (2012) 133–149.
[112] Q. Ma, L. Cheng, F. Gong, Z. Dong, C. Liang, M. Wang, et al., Platinum nanoworms for imaging-guided combined cancer therapy in the second near-infrared window, J. Mater. Chem. B 6 (31) (2018) 5069–5079.
[113] Y. Li, K.-H. Yun, H. Lee, S.-H. Goh, Y.-G. Suh, Y. Choi, Porous platinum nanoparticles as a high-Z and oxygen generating nanozyme for enhanced radiotherapy *in vivo*, Biomaterials 197 (2019) 12–19.
[114] F. Salehi, F. Daneshvar, M. Karimi, R.D. Vais, M. Mosleh-Shirazi, N. Sattarahmady, Enhanced melanoma cell-killing by combined phototherapy/radiotherapy using a mesoporous platinum nanostructure, Photodiagnosis Photodyn. Ther. 28 (2019) 300–307.
[115] H. Gehrke, J. Pelka, C.G. Hartinger, H. Blank, F. Bleimund, R. Schneider, et al., Platinum nanoparticles and their cellular uptake and DNA platination at non-cytotoxic concentrations, Arch. Toxicol. 85 (7) (2011) 799–812.
[116] S. Ramasamy, D. Bennet, S. Kim, Synthesis of hollow mesoporous ruthenium nanoparticles: evaluation of physico-chemical properties and toxicity, RSC Adv. 5 (97) (2015) 79616–79623.
[117] Y. Chen, Y. Yang, B. Xu, S. Wang, B. Li, J. Ma, et al., Mesoporous carbon nanomaterials induced pulmonary surfactant inhibition, cytotoxicity, inflammation and lung fibrosis, J Environ Sci 62 (2017) 100–114.
[118] H. Heli, J. Pishahang, H.B. Amiri, Synthesis of hexagonal CoAl-layered double hydroxide nanoshales/carbon nanotubes composite for the non-enzymatic detection of hydrogen peroxide, J. Electroanal. Chem. 768 (2016) 134–144.
[119] M.S. Hamdy, N.S. Awwad, A.M. Alshahrani, Mesoporous magnesia: synthesis, characterization, adsorption behavior and cytotoxic activity, Mater. Des. 110 (2016) 503–509.
[120] J. Depciuch, M. Stec, B. Klebowski, J. Baran, M. Parlinska-Wojtan, Platinum–gold nanoraspberries as effective photosensitizer in anticancer photothermal therapy, J. Nanobiotechnol. 17 (1) (2019) 107.
[121] Z. Zhou, K. Hu, R. Ma, Y. Yan, B. Ni, Y. Zhang, et al., Dendritic platinum–copper alloy nanoparticles as theranostic agents for multimodal imaging and combined chemophotothermal therapy, Adv. Funct. Mater. 26 (33) (2016) 5971–5978.
[122] Y. Wang, J. Yang, H. Liu, X. Wang, Z. Zhou, Q. Huang, et al., Osteotropic peptide-mediated bone targeting for photothermal treatment of bone tumors, Biomaterials 114 (2017) 97–105.
[123] J. Li, X. Zu, G. Liang, K. Zhang, Y. Liu, K. Li, et al., Octopod PtCu nanoframe for dual-modal imaging-guided synergistic photothermal radiotherapy, Theranostics 8 (4) (2018) 1042.
[124] Y. Deng, X. Tian, S. Lu, M. Xie, H. Hu, R. Zhang, et al., Fabrication of multifoliate PtRu bimetallic nanocomplexes for computed tomography imaging and enhanced synergistic thermoradiotherapy, ACS Appl. Mater. Interfaces 10 (37) (2018) 31106–31113.
[125] A.C. Anselmo, S. Mitragotri, Nanoparticles in the clinic: an update, Bioeng Transl Med 4 (3) (2019), e10143.
[126] F. Chen, W. Cai, Nanomedicine for targeted photothermal cancer therapy: where are we now? Nanomedicine 10 (1) (2015) 1–3.
[127] R. Bawa, Nanoparticle-based therapeutics in humans: a survey, Nanotech. L. & Bus. 5 (2008) 135.
[128] J.L. West, Nano-technologies for biomedical applications, *Conf Proc IEEE Eng Med Biol Soc*. IEEE. (2006) 7–8.
[129] E.S. Day, et al., Nanoshell-mediated photothermal therapy improves survival in a murine glioma model, J. Neuro Oncol. 104 (1) (2011) 55–63.
[130] A.R. Rastinehad, et al., Gold nanoshell-localized photothermal ablation of prostate tumors in a clinical pilot device study, Proc. Natl. Acad. Sci. U. S. A. 116 (37) (2019) 18590–18596.
[131] G. Bort, et al., EPR-mediated tumor targeting using ultrasmall-hybrid nanoparticles: from animal to human with theranostic AGuIX nanoparticles, Theranostics 10 (3) (2020) 1319–1331.
[132] G. Le Duc, et al., Advantages of gadolinium based ultrasmall nanoparticles vs molecular gadolinium chelates for radiotherapy guided by MRI for glioma treatment, Cancer Nanotechnol 5 (1) (2014) 4.